ADVANCED FUNCTIONAL MATERIALS
www.afm-journal.de

Toward One-Way Smoke: Synthesis of Copper-Based Microclubs with Asymmetric Scattering and Absorption

Shichen Guo, Michael Boyarsky, S. Avery Vigil, Yifan Yu, Ivan A. Moreno-Hernandez, Michael E. Gehm, and Benjamin J. Wiley**

The ultimate goal of this work is to create an engineered aerosol that acts as one-way smoke, i.e. it creates an asymmetric vision environment in which the ability to image objects depends on the viewing direction. To this end, a rapid, one-pot synthesis of copper-based microclubs is developed that consists of a Cu_2O octahedron attached to a Cu_2O@Cu shaft. Millions of synthesized particles are analyzed in minutes with a FlowCam to provide a robust statistical analysis of their geometry, and rapidly elucidate the roles of the reaction constituents on the particle shape and yield. The combination of asymmetry in both shape and composition introduces a 30% difference in scattering of light propagating parallel to the microclub axis from opposing directions. This work represents a first step toward the creation of an asymmetric imaging environment with an aerosol consisting of acoustically aligned microclubs.

1. Introduction

Scattering of light within aerosols (e.g., fog or smoke) causes isotropic vision obstruction through random redirection of light.[1,2] If one creates an aerosol in which the magnitude of light scattering differs in opposing directions, such an aerosol has the potential to act as "one-way smoke", i.e. it could enable the smoke to appear transparent in one direction but opaque in the opposing direction. Conventional wisdom is that the creation of one-way smoke is impossible because it would violate Lorentz reciprocity, i.e. that an electromagnetic field should remain unchanged if one interchanges the positions of a light source and detector.[3] However, such reciprocity applies to the extinction cross section (ECS) of a particle, not its scattering cross section (SCS). Recent theoretical results indicate that since extinction is the sum of scattering and absorption, a particle with asymmetric absorption permits asymmetric scattering.[4] However, there are very few experimental demonstrations of particles that exhibit properties that would enable the creation of one-way smoke.[5,6] Previous results indicate that a particle with asymmetric geometry is sufficient to enable asymmetric scattering.[4,5,7–11] We expect that asymmetric scattering could be enhanced by introducing asymmetry in both the particle geometry and material composition. Among various candidate structures, the "matchstick" structure stands out as having a shape and compositional asymmetry that is desired for asymmetric vision.[12–23] These specialized shapes, comprising a distinct "head" and an elongated "shaft," may be tailored to provide the necessary geometric asymmetry in conjunction with specific material properties. The prospect of employing different materials with distinct absorption and scattering characteristics for various components within the matchstick-shaped structure may amplify asymmetric scattering. These possibilities present a promising avenue for exploration in the creation of an asymmetric vision environment.

The pioneering studies on synthesis of matchstick-shaped particles focused on metal-based hybrid nanostructures, such as Co-TiO_2,[14] Au-CdS,[16] AgCdSe-Au,[13] and Ag-Au.[17] These structures were synthesized using a two-step, seed-mediated growth method. In these processes, nanorods served as the seeds and the "head" of the structure grew on one side of the rod, controlled by surfactants,[14,17] UV light,[16] or pH.[13]

SiO_2-based colloidal microparticles constitute another class of matchstick-shaped structures that have been extensively researched.[12,15,18–23] Much like the aforementioned nanostructures, most of these microparticles were synthesized using a two-step, "seeded-growth" method. In these studies, certain colloidal particles (like FeO_X, MnO_X, SiO_2, Ag, and polystyrene) acted as the seeds and the SiO_2 rods grew anisotropically from the water droplets attached to the seeds. Notably, a single group successfully created SiO_2 rods with a small hollow sphere attached to one end using a one-step tetraethoxysilane (TEOS) hydrolysis.[24] However, this structure was only achieved by using TEOS that had been exposed to air for over a year due to partial hydrolysis and condensation of TEOS. Such year-long syntheses are obviously not practical.

S. Guo, S. A. Vigil, Y. Yu, I. A. Moreno-Hernandez, B. J. Wiley
Department of Chemistry
Duke University
Durham, NC 27708, USA
E-mail: benjamin.wiley@duke.edu
M. Boyarsky, M. E. Gehm
Department of Electrical and Computer Engineering
Duke University
Durham, NC 27708, USA
E-mail: michael.gehm@duke.edu

The ORCID identification number(s) for the author(s) of this article can be found under https://doi.org/10.1002/adfm.202315289

DOI: 10.1002/adfm.202315289

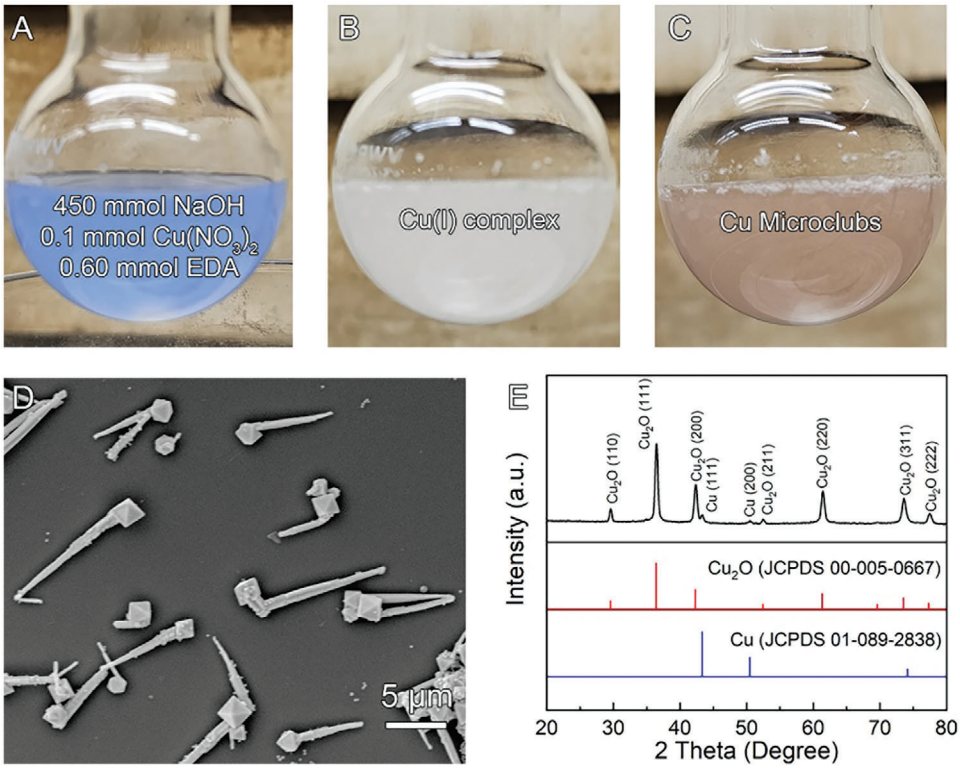

Figure 1. Color changes at different stages of microclub generation. A) The initial mixture before adding N_2H_4, B) the translucent suspension at 5 min, and C) the red-brown color at 20 min. D) SEM image of microclubs. E) Powder XRD of microclubs.

Our group previously studied the growth of copper nanowires on Cu_2O octahedra seeds, leveraging the early formation of Cu_2O nanoparticles in a solution-phase synthesis.[25,26] This previous work established a foundation for the further exploration of copper-based anisotropic structures described herein.

Despite these previous advances, there remains a significant gap in the synthesis of complex micro-sized materials, particularly those with a combination of different components for the head and the shaft. Such two-component structures are a desirable missing piece of the existing particle library because they can enable a higher degree of anisotropic properties. The task of orchestrating the precise formation of such hybrid structures in a single step presents a significant challenge.

In this study, we introduce a novel one-pot synthesis approach for creating two-component, copper-based microclubs with a matchstick shape and asymmetric absorption and scattering properties. We refer to the structure as a "club" rather than a "matchstick" because the "club" moniker seems a better match for its shape, which consists of an octahedral (rather than spherical) Cu_2O "head" and Cu_2O-coated Cu "shaft." Exploiting the reductive properties of hydrazine (N_2H_4) and the oxidation-preventing ability of ethylenediamine (EDA),[27] we are able to generate these distinct microclubs in a highly concentrated sodium hydroxide (NaOH) solution. The high concentration (22.5 M) of NaOH plays a pivotal role in our synthesis, establishing the extreme conditions necessary to form the unique microclub morphology. The morphology of the final product could be adjusted, and its yield optimized, by tuning the concentration of NaOH, N_2H_4, and EDA, a process monitored by a FlowCam (Figure S1, Supporting Information).[28–30] The asymmetric properties of the microclub structure were found by simulation to create a 30% difference in scattering in opposing directions. The innovative method simplifies the synthesis and characterization process, eliminating the need for multiple steps or seed preparation, and offers an efficient pathway for the production of two-component, anisotropic copper-based microstructures with potential to be used for asymmetric vision applications.

2. Results and Discussion

The microclubs were synthesized via a modified hydrazine-reduction method, which was previously utilized in the synthesis of Cu nanowires and Cu_2O octahedra.[25,31] The color evolution of the reaction mixture over time is depicted in **Figure 1**A–C. The initial mixture in Figure 1A comprises 20 mL of a 22.5 M NaOH aqueous solution, 1 mL of a 0.1 M $Cu(NO_3)_2$ aqueous solution, and 40 μL (0.60 mmol) of EDA. The blue color is attributed to a $[Cu(OH)_4]^{2-}$ complex, which typically forms in concentrated NaOH solutions.[25] As the saturation point of a NaOH solution at room temperature is ≈19 M, to prevent precipitation, the 22.5 M NaOH solution was maintained at 50 °C before being used for the reaction.[32]

After preheating the solution in Figure 1A for 5 min in a 50 °C water bath, 10 μL of N_2H_4 was quickly introduced into the solution. The solution turned cloudy white within 10 s due to N_2 generation resulting from the oxidation of N_2H_4 and the simultaneous reduction of $[Cu(OH)_4]^{2-}$ to the colorless $[Cu(OH)_2]^-$. As the bubbles exited the flask, the solution gradually transitioned

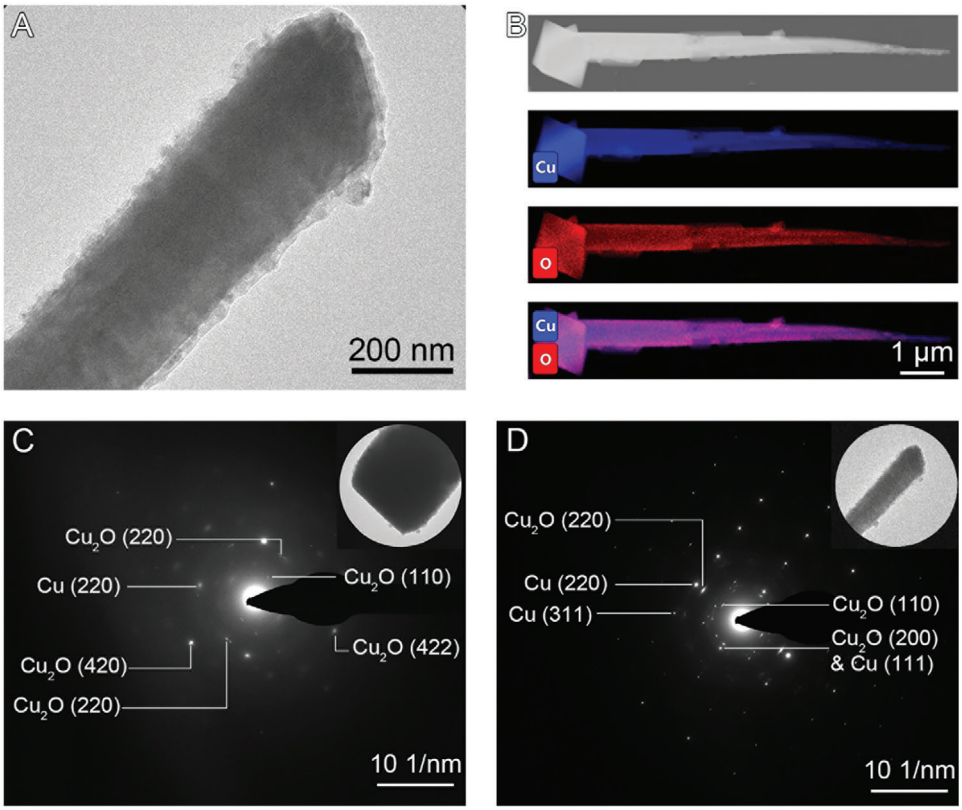

Figure 2. A) HRTEM image of the tip of microclub, B) STEM-EDS mapping of microclub, C) HRTEM and SAED of the octahedral "head" of microclub, D) HRTEM and SAED of the conical "shaft" of microclub.

to a translucent suspension in 5 min (Figure 1B). Subsequently, this suspension shifted to a red-brown color and became darker (Figure 1C). The reaction was stopped at 20 min and the optimal yield of Cu microclubs was obtained.

The morphology of the microclub is evident in the scanning emission microscopy (SEM) image in Figure 1D. Each microclub, synthesized through a one-pot method, features an octahedral "head" and a conical "shaft". X-ray diffraction (XRD) of microclubs demonstrates they consist of both Cu and Cu_2O (Figure 1E). To further determine the structure of microclubs, a detailed compositional analysis was performed with transmission electron microscopes (TEM) (**Figure 2**). The picture of the tip of the microclub suggests it consists of a ≈250 nm-wide Cu core and 25 nm-thick Cu_2O shell (Figure 2A). STEM-EDS mapping results affirm that both the "head" and "shaft" consist of Cu and O elements (Figure 2B). Selected area electron diffraction (SAED) indicates that both the "head" and the "shaft" projections of the microclub are composed of Cu_2O and Cu (Figure 2C,D). As octahedron is typically the structure of Cu_2O (Figure S2, Supporting Information),[25,26] the existence of Cu diffraction in "head" may come from the junction of "head" and "shaft". We also notice that several diffraction spots in Figure 2D cannot be conclusively attributed to either Cu_2O or Cu. Due to the weak peak and lack of additional evidence supporting its existence, we will not delve further here. The presence of Cu_2O and Cu was further corroborated by an etching process, in which Cu_2O was dissolved in glacial acetic acid. The resulting change indicated that both the "head" and "shaft" were partially eroded after 10 min and only the metallic Cu nanowire core was left after 30 min (Figure S3, Supporting Information). These findings all indicate that the octahedral "head" of the microclub is Cu_2O, and the conical "shaft" is Cu coated with Cu_2O, proving that the microclubs are composed of two components that formed in a single reaction.

To gain a deeper understanding of the microclub growth during the one-pot synthesis, we conducted the reaction at various time intervals and investigated the effects of key conditions – NaOH, temperature, N_2H_4, and EDA – on the formation of the microclubs. In order to examine these effects, we utilized SEM to assess morphological changes and a FlowCam (Yokogawa Fluid Imaging Technologies, Figure S1, Supporting Information) to quantify both yield and length variations. The FlowCam is a relatively new instrument that is beginning to be used to accelerate the morphological analysis of particles and microorganisms but has yet to be widely employed in the field of colloidal synthesis.[28–30,33–39] The FlowCam uses flow imaging microscopy for the rapid acquisition of particle images, in conjunction with VisualSpreadsheet 6 software for rapid analysis of 39 geometric parameters (e.g., edge gradient, length, width, aspect ratio). Flow imaging microscopy digitally captures particles by streaming a particle-containing liquid through a microscope. It uses strobed illumination and short shutter speeds to "freeze" moving particles, allowing thousands of sharp images to be captured per second. The software then isolates and stores the particle images from each frame for further analysis. Despite some limitations,

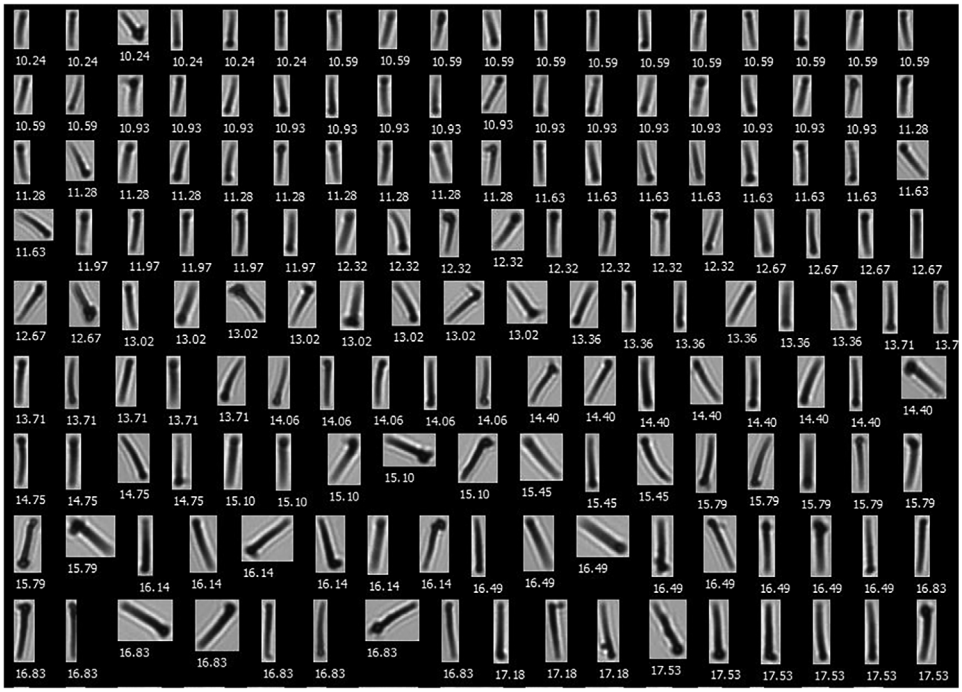

Figure 3. The FlowCam image library used for determining the yield of microclubs in a larger population (100k+) of particles. The number below each particle is the length of microclub (in μm).

FlowCam analysis shows many advantages compared to traditional particle size analysis with TEM/SEM[40–42] (see Table S1, Supporting Information for pros and cons). During each measurement, we acquired a total of 100 000 particle images and filtered out unfocused and background particles. We identified the microclubs within the overall particle population using a prebuilt library that contained 426 preselected microclub images (**Figure 3**). The yield is defined as the ratio of the microclub count to the total particle count.

Figure S4 (Supporting Information) captures the time evolution process of microclub growth. Within the first 5 min, the solution predominantly contains small spherical particles with a diameter of 0.28 ± 0.03 μm (Figure S4A, Supporting Information), corresponding to the near-zero yield of microclubs from the FlowCam analysis. At 10 min, a noticeable transition occurred, as evidenced by the jump in yield to 10% and the emergence of observable microclub structures Figure S4B, Supporting Information) with an average length of 6.69 ± 1.61 μm. This indicates a shift from nucleation to a growth phase, where the small spherical particles have evolved into elongated microclubs. The microclub formation and growth continued until 20 min when the yield increased to 64% and the length to 9.82 ± 3.48 μm (Figure S4C, Supporting Information). A prolonged reaction time beyond 20 min did not promote further microclub formation. At 30 min, the length increased to 10.88 ± 3.66 μm while the yield is similar to that at 20 min (60%). Leaving the reaction to 60 min resulted in a reduced yield (34%) and length (9.99 ± 3.86 μm). During this stage, the precursor appeared to be exhausted, and N_2H_4 continued to reduce Cu_2O to Cu, as evidenced by the progressively irregular shape of microclubs (Figure S4D,E, Supporting Information).

Following the investigation of the time-dependent evolution of microclub growth, we then turned our attention to the role of key conditions in the process, with the first focus on NaOH due to its extremely high concentration in the microclub synthesis (Figure S5, Supporting Information). At lower NaOH concentrations (15 and 17.5 M), the predominant structure was the Cu_2O octahedra with an edge length of ≈1.6 μm (Figure S5B, Supporting Information), and the yield of microclubs measured from the FlowCam was zero. However, a shift occurred when the NaOH solution was supersaturated (20 and 22.5 M). Under these conditions, microclubs started to emerge, underscoring the crucial influence of extremely high NaOH concentrations on the formation of these structures. We hypothesized that higher NaOH concentrations augment the reducing power of N_2H_4 sufficiently to convert Cu(II) to both Cu(I) and Cu(0). This theory is supported by the prolonged duration of the white cloudy state observed in a 22.5 M NaOH solution compared to that in a 15 M NaOH solution, indicating more extensive decomposition of N_2H_4. We also observed that while the lengths of the microclubs formed at 20 and 22.5 M were similar, the yields showed a significant difference (32% vs 64%). This suggests that NaOH may primarily influence the nucleation process, i.e. the initial formation of the microclubs, and the transformation from octahedron to microclub morphology. Once the microclubs begin to form, the length might be largely dictated by other factors in the reaction, such as the reaction time. We found it impossible to increase the NaOH concentration further, such as to 25 M, due to the inability of NaOH to fully dissolve at 50 °C.

To delve deeper into the influence of temperature on microclub formation, beyond its role in the dissolution of highly concentrated NaOH, we also examined how different reaction

temperatures affect both the yield and the length of the microclubs produced. As illustrated in Figure S6A (Supporting Information), the optimum yield was recorded at 50 °C, with deviations from this temperature – either higher or lower – resulting in a decreased yield. At lower temperatures (Figure S6B, Supporting Information), the reaction predominantly yielded a mix of microclubs and particles, indicative of conditions that favor the formation of the Cu(I) product. Conversely, at higher temperatures (Figure S6C, Supporting Information), a shift towards the formation of more irregular or rod-like particles was observed, suggesting a reaction environment conducive to the production of Cu(0). This shift can be attributed to the fact that higher temperatures furnish the necessary energy for the reduction process to advance further towards the generation of Cu(0). In our experiments, maintaining a balanced temperature, specifically at 50 °C, was found to be crucial for the successful formation of two-component microclubs.

We then examined the effect of varying the N_2H_4 amount on the morphology, yield, and length of the microclubs, given its key role as a reducing agent (Figure S7, Supporting Information). The maximum yield and length were attained with 10 µL of N_2H_4. Deviations from this amount resulted in a lower yield and shorter microclub lengths. However, the underlying reasons for these observations differed depending on whether the N_2H_4 volume was increased or decreased. When the amount of N_2H_4 was reduced to 5 µL, microclubs could still form (Figure S7B, Supporting Information), but the yield and length decreased. We attribute this to the reduced amount of N_2H_4 leading to insufficient reducing power for optimal microclub formation and growth. On the other hand, increasing the volume of N_2H_4 led to a decrease in yield and length due to over-reduction of Cu(II) to Cu(0). This theory is supported by the observation of numerous rod-like and irregular particles present in the product. (Figure S7C, Supporting Information).

The final key reactant is EDA. EDA plays an important role in suppressing the nucleation of Cu_2O nanostructures. Figure S8A (Supporting Information) shows that the maximum yield was achieved with 0.6 mmol of EDA. Either increasing or decreasing the amount of EDA would lead to shorter microclubs and more impurities, which were mainly attributed to the formation of small Cu_2O particles (Figure S8B,C, Supporting Information). At 0 mmol of EDA (Figure S8B, Supporting Information), nucleation of Cu_2O seeds was rapid and many small particles formed in the early stage of the reaction. However, the suppression of oxide formation was not sufficient to enable the formation of a high yield of microclubs after 20 min. At concentrations of EDA higher than the optimum, fewer nuclei were generated and fewer small particles were observed in the final product (Figure S8C, Supporting Information). At even higher concentrations of EDA (3.75 mmol), the nucleation of Cu_2O was completely suppressed, the solution remained translucent after 20 min, and no particles were observed with SEM and the FlowCam. Therefore, 0.6 mmol of EDA represented the optimum concentration for sufficient suppression of copper oxidation to enable nucleation of Cu_2O particles and subsequent growth of microclubs.

To analyze the anisotropic optical properties of the microclubs, the structure was simulated in CST Studio with plane wave incidence at 60 THz, or 5 µm. To simplify the structure for simulation, the octahedron was set as Cu_2O with dielectric constant of 11.54[43] and an edge length of 2 µm. The shaft was set to be Cu with a conductivity of 5.8×10^7 S m^{-1},[44] a length of 8 µm, and a radius that goes from 0.8 to 0.3 µm along the shaft. **Figure 4A** shows the plane wave incidence, as well as the rotation of the microclub structure.

The microclub exhibits anisotropic scattering and absorption properties that may contribute towards the creation of an asymmetric scattering environment. The lossy scattering and absorption of the structure vary as a function of incident angle. Though the scattering and absorption of the 90- and 270-degree rotations are mirror images of each other, the microclub exhibits anisotropic optical properties between the 0- and 180-degree rotations. This behavior can be seen in Figure 4A by the differences between the magnitude and shape of the scattering profile and can be seen in Figure 4B,C and Table S2 (Supporting Information) by the differences in the absorption cross section (ACS) and SCS in opposing directions (e.g., ACS for the 0-degree rotation is 50% larger than for the 180-degree rotation).

To leverage this behavior, the microclubs could be deployed and acoustically aligned in a cloud between two observers. In such an environment, we expect that propagation of light through the cloud along the direction with greater scattering would result in greater deflection and diffusion of light, resulting in a blurry, low-contrast image that makes it difficult to resolve objects. In the other direction, however, we expect greater attenuation of propagating light that would reduce the signal but retain, rather than randomize, spatial information and enable resolution of objects. In this way, the extinction in the two directions remains consistent, but the impact on imaging varies, enabling the practical creation of an asymmetric imaging environment in the infrared.

3. Conclusion

The successful synthesis of two-component, copper-based microclubs with a simple one-pot approach represents a significant step towards the creation of engineered aerosols that act as one-way smoke. The unique synthesis process leverages the reductive properties of N_2H_4 and the oxidation-inhibiting properties of EDA in a highly concentrated NaOH solution, allowing for the creation of this anisotropic structure without the need for templates, seeds, or multiple steps. Additionally, the FlowCam expedites the statistical analyses of particle count and geometric properties, rapidly enabling an understanding of how the time and reagent concentration influence the product yield and morphology. Simulations of the anisotropic microclub structure indicate the structure will exhibit a 30% difference in scattering in the magnitude of scattering for light propagating parallel to the microclub axis from opposing directions. This showcases the potential for a cloud of oriented microclub particles to create an asymmetric vision environment. Future work will focus on an experimental demonstration of vision asymmetry.

4. Experimental Section

Materials: Sodium hydroxide (NaOH, pellets, 97%) was purchased from VWR. Copper(II) nitrate hemi(pentahydrate) ($Cu(NO_3)_2{\cdot}2.5H_2O$, 98%), ethylenediamine (EDA, 99%), hydrazine solution (N_2H_4, 35 wt.% in H_2O), methanol (99.8%), polyvinylpyrrolidone (PVP, MW = 10 000) were

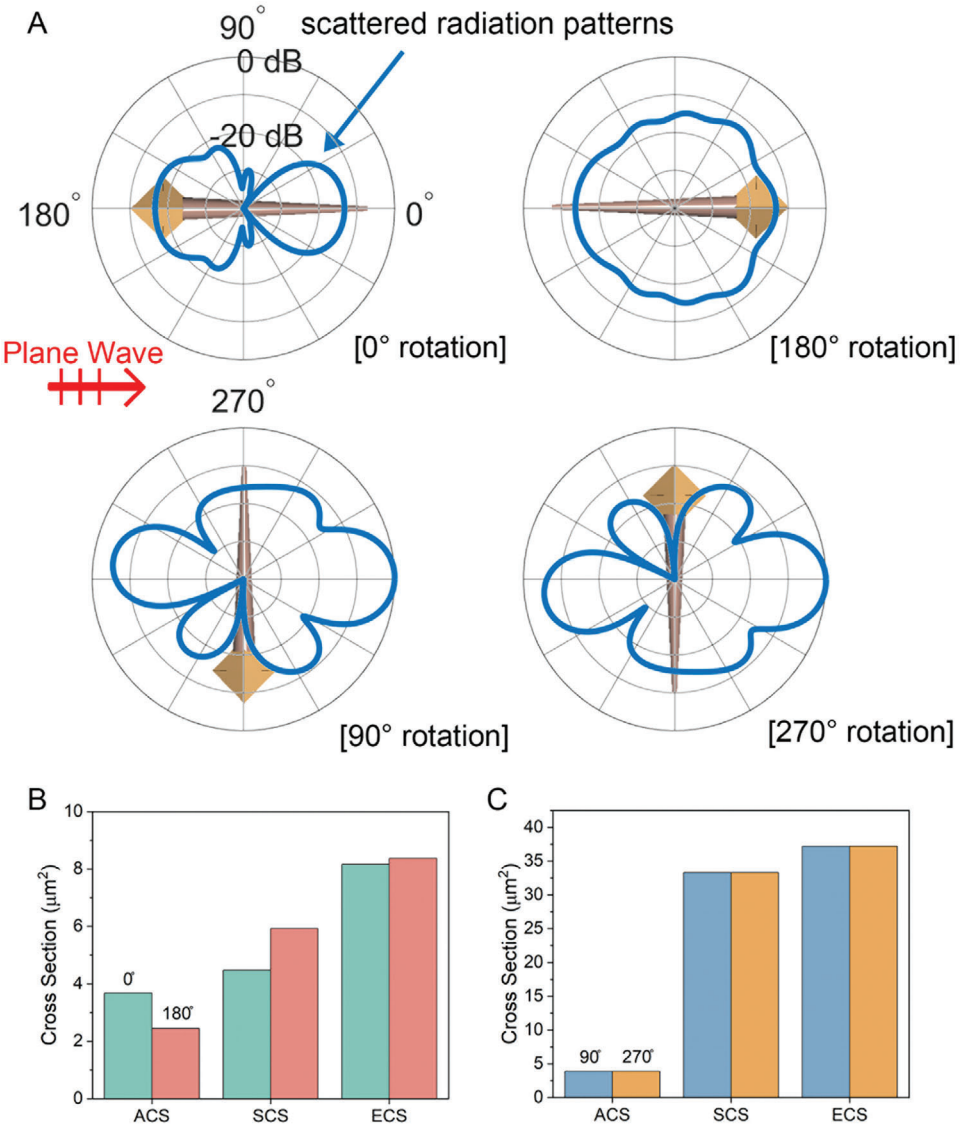

Figure 4. A) Electromagnetic simulation results for the microclub structure illuminated with a plane wave incident toward the 0-degree direction. The structure was simulated in CST Studio for the four principal rotations, [0, 180] degree rotations for anisotropic orientations (top two) and [90, 270] degree rotations for broadside orientations (bottom two), respectively. The scattered radiation patterns were normalized to the maximum value among all rotations and plotted as a function of output angle. B) Absorption cross section (ACS), scattering cross section (SCS), and extinction cross section (ECS) of the microclub structure at 0- and 180-degree rotations. C) ACS, SCS, and ECS comparison at 90- and 270-degree rotations.

purchased from Sigma–Aldrich. Benzotriazole (99%) was purchased from Acros Organics. N,N-diethylhydroxylamine (DEHA, 98%) was purchased from Santa Cruz Biotechnology. All reagents were used as received.

One-Pot Synthesis of Copper-Based Microclubs: NaOH aqueous solution (22.5 M) was first prepared by fully dissolving NaOH in a polypropylene bottle or centrifuge tube. This solution was then stored in an oven at 50 °C to prevent precipitation at room temperature. For the synthesis, NaOH (22.5 M, 20 mL), $Cu(NO_3)_2{\cdot}2.5H_2O$ (0.1 M, 1 mL), and EDA (0.60 mmol, 40 μL) were first mixed in a 50 mL round bottle flask and preheated in a 50 °C water bath for 5 min with continuous stirring at 700 rpm. N_2H_4 was then quickly added into the solution and the reaction turned cloudy white within 5 s. The reaction was terminated after 20 min when the solution turned red-brown and the solution was transferred to a centrifuge tube containing 3% PVP and 1% DEHA aqueous solution (≈10 mL). The mixture was vortexed vigorously and the products floated on the surface as brown aggregations. The products were then collected by draining the liquid and washed with deionized water and methanol several times by centrifuging at 2000 rpm for 10 min. For short-term storage, the products were dispersed in either 1% DEHA solution or pure methanol. For long-time storage, the products were dispersed in an aqueous solution containing 0.5 wt.% benzotriazole to prevent corrosion.[45]

Instrumentation and Characterization: The microclubs were characterized by scanning electron microscopy (SEM, Thermo Scientific Apreo S model), scanning transmission electron microscopy (STEM, ThermoFisher Titan 80–300), high-resolution transmission electron microscopy (HRTEM, FEI Tecnai G^2 Twin), X-ray diffraction (XRD, Panalytical X'Pert PRO MRD HR XRD System), and flow imaging microscopy (FIM).

HRTEM data were collected on an FEI Tecnai G^2 Twin microscope operated at 200 kV with an exposure time of 2 s and a resolution of 4096 × 4096 pixels. Electron diffraction data were collected with an exposure time of 4 s and an observed camera length of 285 mm. Selected area electron diffraction was utilized to isolate the "head" of the microclub and the "shaft" of

the microclub, allowing the elucidation of the differing chemical compositions. Electron diffraction data were analyzed in the Crystalmaker SingleCrystal program, using a known system to ensure correct camera length calibrations. Peaks were assigned using powder diffraction rings generated from CIFs loaded directly into the program. STEM-EDS data were collected on a ThermoFisher Titan 80–300 scanning transmission electron microscope operated at 200 kV at the Analytical Instrumentation Facility at NC State University using an FEI double tilt holder with a molybdenum retention clip. The EDS map in Figure 2B was collected with a dwell time of 32 us at a resolution of 833 × 148 pixels over 94 frames. The resulting EDS maps were analyzed in ThermoFisher's Velox program using the net% analysis mode with pre- and post-filtering enabled.

The yield and length of microclub were determined via FIM. FIM, a dynamic image analysis technique, can provide particle sizes, counts, and morphology within a few minutes. The FIM measurements were conducted using a FlowCam (FlowCam 8000, Yokogawa Fluid Imaging Technologies) equipped with a 20X objective lens, an 80 µm FOV flow cell, and a 0.5 mL syringe pump. In each test run, ≈0.5 mL of diluted microclub solution was added to the FlowCam. The system automatically captured images of the particles at a flow rate of 0.05 mL min^{-1} and an auto-imaging rate of 27 frames per second. The stop condition was when particle count reached 100 000. Two filters were applied to determine the total particle count and microclub count. The first filter was the value filter with an edge gradient between 150 and 255 to exclude unfocused and background particles. The second filter was the statistical filter from a pre-built library with 426 preselected microclub images to identify microclubs amongst the overall particle population. Upon applying the filters, the software directly provided the particle count and size. The yield of microclub was then calculated using the following equation: Yield = Microclub count / Total particle count.

Supporting Information

Supporting Information is available from the Wiley Online Library or from the author.

Acknowledgements

The authors would like to gratefully acknowledge financial support from the Defense Advanced Research Projects Agency (DARPA) as part of the "Coded Visibility" program (Prime Contract FA8650-22-C-7210). This work was performed in part at the Duke University Shared Materials Instrumentation Facility (SMIF) and Analytical Instrumentation Facility (AIF) at North Carolina State University, the members of the North Carolina Research Triangle Nanotechnology Network (RTNN), which is supported by the National Science Foundation (award number ECCS-2025064) as part of the National Nanotechnology Coordinated Infrastructure (NNCI). S.A.V. acknowledges a National Science Foundation Research Grant Fellowship under Grant No. DGE-2139754.

Conflict of Interest

The authors declare no conflict of interest.

Data Availability Statement

The data that support the findings of this study are available in the supplementary material of this article.

Keywords

anisotropic growth, asymmetric scattering, copper, microclub, one-pot synthesis

Received: December 1, 2023
Revised: March 1, 2024
Published online: March 17, 2024

[1] M. Tanzid, N. J. Hogan, H. Robatjazi, A. Veeraraghavan, N. J. Halas, *J. Opt.* **2018**, *20*, 054001.
[2] M. Tanzid, N. J. Hogan, A. Sobhani, H. Robatjazi, A. K. Pediredla, A. Samaniego, A. Veeraraghavan, N. J. Halas, *ACS Photonics* **2016**, *3*, 1787.
[3] V. S. Asadchy, M. S. Mirmoosa, A. Díaz-Rubio, S. Fan, S. A. Tretyakov, *Proc. IEEE* **2020**, *108*, 1684.
[4] D. L. Sounas, A. Alù, *Opt. Lett.* **2014**, *39*, 4053.
[5] L. Yuan, C. Zhang, X. Zhang, M. Lou, F. Ye, C. R. Jacobson, L. Dong, L. Zhou, M. Lou, Z. Cheng, P. M. Ajayan, P. Nordlander, N. J. Halas, *Nano Lett.* **2019**, *19*, 4413.
[6] A. F. da Mota, M. M. Sadafi, H. Mosallaei, *Sci. Rep.* **2024**, *14*, 3850.
[7] P. Dhindsa, D. Solti, C. R. Jacobson, A. Kuriakose, G. N. Naidu, A. Bayles, Y. Yuan, P. Nordlander, N. J. Halas, *Nano Lett.* **2022**, *22*, 10088.
[8] T. Tumkur, X. Yang, C. Zhang, J. Yang, Y. Zhang, G. V. Naik, P. Nordlander, N. J. Halas, *Nano Lett.* **2018**, *18*, 2040.
[9] C. R. Jacobson, G. Wu, L. B. Alemany, G. N. Naidu, M. Lou, Y. Yuan, A. Bayles, B. D. Clark, Y. Cheng, A. Ali, A.-L. Tsai, I. A. Tonks, P. Nordlander, N. J. Halas, *Nano Lett.* **2022**, *22*, 5570.
[10] B. D. Clark, C. R. Jacobson, M. Lou, J. Yang, L. Zhou, S. Gottheim, C. J. DeSantis, P. Nordlander, N. J. Halas, *Nano Lett.* **2018**, *18*, 1234.
[11] M. Yorulmaz, A. Hoggard, H. Zhao, F. Wen, W.-S. Chang, N. J. Halas, P. Nordlander, S. Link, *Nano Lett.* **2016**, *16*, 6497.
[12] X. Li, T. Zhao, Y. Lu, P. Wang, A. M. El-Toni, F. Zhang, D. Zhao, *Adv. Mater.* **2017**, *29*, 1701652.
[13] S. Liang, X. L. Liu, Y. Z. Yang, Y. L. Wang, J. H. Wang, Z. J. Yang, L. B. Wang, S. F. Jia, X. F. Yu, L. Zhou, J. B. Wang, J. Zeng, Q. Q. Wang, Z. Zhang, *Nano Lett.* **2012**, *12*, 5281.
[14] M. Casavola, V. Grillo, E. Carlino, C. Giannini, F. Gozzo, E. F. Pinel, M. A. Garcia, L. Manna, R. Cingolani, P. D. Cozzoli, *Nano Lett.* **2007**, *7*, 1386.
[15] X. Zhang, W. Xie, H. Wang, Z. Zhang, *Chem. Commun.* **2021**, *57*, 3797.
[16] L. Carbone, A. Jakab, Y. Khalavka, C. Sönnichsen, *Nano Lett.* **2009**, *9*, 3710.
[17] F. Wang, S. Cheng, Z. Bao, J. Wang, *Angew. Chem. Int. Ed. Engl.* **2013**, *52*, 10344.
[18] B. W. Longbottom, L. A. Rochford, R. Beanland, S. A. Bon, *Langmuir* **2015**, *31*, 9017.
[19] A. R. Morgan, A. B. Dawson, H. S. McKenzie, T. S. Skelhon, R. Beanland, H. P. W. Franks, S. A. F. Bon, *Mater. Horiz.* **2014**, *1*, 65.
[20] B. Zhao, H. Zhou, C. Liu, Y. Long, G. Yang, C.-H. Tung, K. Song, *New J. Chem.* **2016**, *40*, 6541.
[21] D. R. Hayden, C. L. Kennedy, K. P. Velikov, A. van Blaaderen, A. Imhof, *Langmuir* **2019**, *35*, 14913.
[22] Y. Gao, R. P. A. Dullens, D. Aarts, *Soft Matter* **2018**, *14*, 7119.
[23] B. Zhao, D. Li, Y. Long, K. Song, *Sci. Rep.* **2019**, *9*, 8591.
[24] F. Hagemans, R. K. Pujala, D. S. Hotie, D. M. E. Thies-Weesie, D. A. M. de Winter, J. D. Meeldijk, A. van Blaaderen, A. Imhof, *Chem. Mater.* **2019**, *31*, 521.
[25] S. Ye, A. R. Rathmell, Y. C. Ha, A. R. Wilson, B. J. Wiley, *Small* **2014**, *10*, 1771.
[26] S. Alvarez, S. Ye, P. F. Flowers, B. J. Wiley, *Chem. Mater.* **2015**, *27*, 570.
[27] M. J. Kim, P. F. Flowers, I. E. Stewart, S. Ye, S. Baek, J. J. Kim, B. J. Wiley, *J. Am. Chem. Soc.* **2017**, *139*, 277.
[28] Y. H. Lee, Y. Kwon, C. Kim, Y.-E. Hwang, M. Choi, Y. Park, A. Jamal, D.-Y. Koh, *JACS Au* **2021**, *1*, 1198.
[29] S. A. Hice, M. Varona, A. Brost, F. Dai, J. L. Anderson, B. F. Brehm-Stecher, *Anal. Bioanal. Chem.* **2020**, *412*, 1741.

[30] A. S. Sediq, S. K. D. Waasdorp, M. R. Nejadnik, M. M. C. van Beers, J. Meulenaar, R. Verrijk, W. Jiskoot, *Pharm. Res.* **2017**, *34*, 1104.
[31] A. R. Rathmell, S. M. Bergin, Y.-L. Hua, Z.-Y. Li, B. J. Wiley, *Adv. Mater.* **2010**, *22*, 3558.
[32] M. Hellström, J. Behler, *Phys. Chem. Chem. Phys.* **2017**, *19*, 82.
[33] H. Nishiumi, N. Deiringer, N. Krause, S. Yoneda, T. Torisu, T. Menzen, W. Friess, S. Uchiyama, *J. Pharm. Sci.* **2022**, *111*, 3017.
[34] H. Shibata, A. Harazono, M. Kiyoshi, A. Ishii-Watabe, *J. Pharm. Sci.* **2022**, *111*, 648.
[35] A. D. Grabarek, W. Jiskoot, A. Hawe, K. Pike-Overzet, T. Menzen, *Eur. J. Pharm. Biopharm.* **2021**, *167*, 38.
[36] A. L. Daniels, C. P. Calderon, T. W. Randolph, *Biotechnol. Bioeng.* **2020**, *117*, 3322.
[37] K. B. Cook, A. Belcher, D. B. Juez, G. Stowasser, S. Fielding, R. A. Saunders, M. A. Elsafi, G. A. Wolff, S. J. Blackbird, G. A. Tarling, D. J. Mayor, *Deep Sea Res. Part II* **2023**, *210*, 105296.
[38] J. d. C. L. d. Rosa, T. d. S. Matos, D. C. B. da Silva, C. Reis, C. d. O. Dias, T. U. P. Konno, L. D. d. A. Fernandes, *Diversity* **2023**, *15*, 637.
[39] S. M. Burns, R. M. Bundy, W. Abbott, Z. Abdala, A. R. Sterling, P. D. Chappell, B. D. Jenkins, K. N. Buck, *Limnol. Oceanogr.* **2023**, *68*, 525.
[40] L.-Q. Guan, S. Shi, X.-W. Niu, S.-C. Guo, J. Zhao, T.-M. Ji, H. Dong, F.-Y. Jia, J.-W. Xiao, L.-D. Sun, C.-H. Yan, *Adv. Sci.* **2022**, *9*, 2201354.
[41] M. Ge, F. Su, Z. Zhao, D. Su, *Mater. Today Nano* **2020**, *11*, 100087.
[42] H. Cai, E. G. Xu, F. Du, R. Li, J. Liu, H. Shi, *Chem. Eng. J.* **2021**, *410*, 128208.
[43] I. Petousis, D. Mrdjenovich, E. Ballouz, M. Liu, D. Winston, W. Chen, T. Graf, T. D. Schladt, K. A. Persson, F. B. Prinz, *Sci. Data* **2017**, *4*, 160134.
[44] C. Christopoulos, *Principles and Techniques of Electromagnetic Compatibility*, CRC Press, Boca Raton **2022**.
[45] M. Finšgar, I. Milošev, *Corros. Sci.* **2010**, *52*, 2737.

